Bulletin of the Seismological Society of America. Vol. 67, No. 3, pp. 677-691. June 1977

MODELING CRUSTAL STRUCTURE THROUGH THE USE OF CONVERTED PHASES IN TELESEISMIC BODY-WAVE FORMS

By L. J. Burdick and Charles A. Langston

ABSTRACT

By comparing records of the radial component of motion of teleseismic *P* waves to records of the vertical component, it is possible to identify *S* phases within the *P* wave form. These phases are generated by the mechanism of *P* to *S* conversion at discontinuities in velocity under the receiving station. Similar phases of the *S* to *P* converted type appear as precursors to the direct *SV* arrival. Models for the crustal structure can be tested by generating synthetic seismograms for both components of motion of both the *P* and *SV* waves and comparing with the data. The technique has been used to model the crustal structure at WWSSN stations CAR and COR. It has also been used to check a recently proposed model for the crustal structure in eastern Canada which contains a large low-shear-velocity zone at the base of the crust. This study indicates that the crustal structure in eastern Canada is highly non-uniform with perhaps few features common to the whole region. Finally, the technique is used to identify several stations in the WWSSN which appear to be located on highly anomalous structure.

Introduction

The displacement at the Earth's surface due to the arrival of a teleseismic body wave is affected by a number of unknown quantities. These include the source time function, the Earth's velocity structure near the source, the velocity structure near the turning point of the ray, and the crust and upper mantle structure under the observation point. A number of techniques have been developed to separate the effects of the structure under the observation point from the others and to translate this information into models for the crust and upper mantle. One method involves the use of synthetic seismograms to model S to P converted phases from the Mohorovičić discontinuity (Båth and Stefansson 1966; Jordan and Frazer, 1975). An attractive feature of this technique is that it is simple and unambiguous. A specific arrival in the wave train is associated with a specific discontinuity in the Earth. Until now, the method of using synthetic seismograms has been limited to studies of $S - P$ phases from the moho. However, the moho or any other boundary which produces an S to P converted phase strong enough to be used in a study of this type will produce strong reflections and conversions of other kinds as well. Some of these can be identified quite readily within the P wave form. The purpose of this paper will be to demonstrate that all types of converted phases can be used together to obtain a reliable model of the crustal structure. A second method of determining the receiver structure involves modeling the ratio of the Fourier spectral amplitude of the vertical displacement to the spectral amplitude of the horizontal displacement of incoming P waves. The theoretical basis for this type of analysis has been discussed by Phinney (1964), Hannon (1964), Kurita (1973a), Leblanc (1967), and Fernandez (1967). The technique has been used to model receiver structures by Fernandez and Careaga (1968), Bonjer *et al.* (1970), Kurita (1973b), and Leong (1975) among others. The main advantage of this technique is that it does not require a knowledge of the incident

wave form. Its disadvantages are that it lacks the stability and ease of interpretation of comparing time-domain synthetic seismograms directly to the data.

Reflected and Converted Phases in the *P* Wave Form

For a plane *P* wave incident at the base of the crust there will be five phases which are first-order in reflection or transmission coefficients at the moho. In the notation of Båth and Stefánnson (1966) these are *PpPmp PpSmp, Ps, PpPms* and *PpSms*. The first two of these are difficult to observe because they are small and are generally washed out by the strong interaction of the instrument with the direct arrival. The third phase *Ps* arrives only seconds behind the direct arrival and unless it is unusually strong it is also hard to identify. The last two phases, however, can often be observed in the radial component of motion of teleseismic *P* waves. At an epicentral range of say 60°, a *P* wave will have an incident angle at the free surface of about 22°. Only 37 per cent of the total amplitude appears on the radial component. To conserve phase velocity, a *P* to *S* converted phase must have an incident angle of about 12°. Ninety-eight per cent of its total amplitude will appear on the radial component. The converted phase will be enhanced with respect to the direct arrival on the radial component by a factor of nearly 3. This makes these phases much easier to identify particularly if the vertical component of motion is used as a visual guide as to what the motion on the radial component would be if there were no *S* waves present.

Even though these phases can be seen as a clear difference in the radial and vertical signals, they are difficult to model if the vertical component is still changing rapidly when they arrive. This could be caused by a long duration, multicomponent source, interaction of a shallow source with the free surface, or a secondary arrival from a sharp discontinuity near the turning point of the ray. To avoid these difficulties it is advantageous to use observations of deep earthquakes ($h \sim 600$ km) of intermediate size at epicentral ranges of 30° to 80°. The incident time function for events of this type can often be modeled as a single unidirectional pulse of about 2 or 3 sec duration. The instrument response of a long-period, 15–100 or 30–90, instrument to this type of arrival is nearly over by the time that the *PpPms* and *PpSms* phases for a typical crust arrive. It is still generally necessary, however, to compute synthetic seismograms in the manner of Jordan and Frazer (1975) to correctly analyze the relative amplitudes. Equating relative trace amplitudes to relative arrival amplitudes as did Båth and Stefánnson (1966) would not work well since the two phases interact with each other and with other late arrivals.

Computation of Synthetic Seismograms

The techniques for computing synthetic seismograms have been outlined by Langston and Helmberger (1975) and Mikumo (1971) among others. The trace amplitude A as a function of time can be written

$$A(t) = I(t)*Q(t)*S(t)*R(t).$$

I is the appropriate instrument response, Q the Futterman (1962) Q operator evaluated at $T/Q = 0.75$ for incident P waves and $T/Q = 3.0$ for incident S waves, S the source time function, R the earth response and $*$ the convolution operator. In most of the cases considered here, we will model the source pulse as a trapezoid with three adjustable time parameters δt_1, δt_2 and δt_3 as proposed in Langston and Helmberger (1975). In a few cases where the source appears to be a double event, the pulse

will be modeled as a sum of two trapezoids. An appropriate model can be rapidly determined by deconvolving the theoretical Q and instrument responses from the observed vertical P wave form and fitting a trapezoid to the result by inspection. The earth response at ranges between 30° and 80° for a deep earthquake is essentially only the response of the structure under the receiver since the near source and turning point earth structure have very little effect. R can be computed either by using a ray expansion or the Haskell (1960, 1962) propagator matrix technique. The latter is more convenient and will be used to compute the synthetic seismograms presented in this paper. However, it is also enlightening to associate certain peaks in the record with waves that travel along certain specified paths. Therefore, we will continue to discuss these peaks in terms of rays.

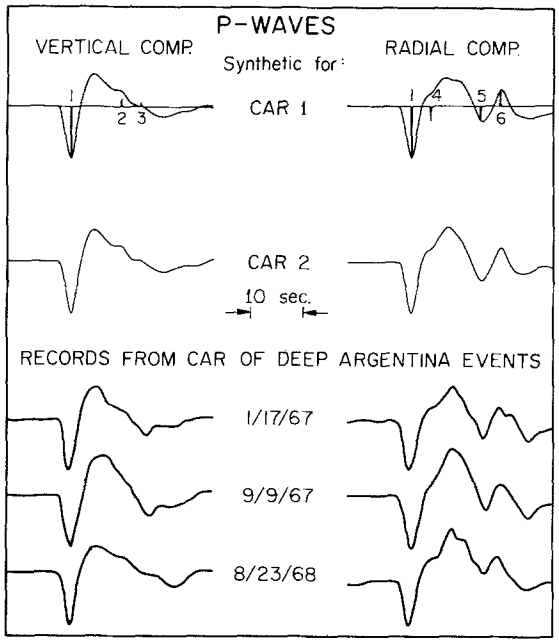

FIG. 1. The radial components of motion at WWSSN station CAR are shown on the *right* for comparison with the vertical components on the *left*. The *top two records* in light line are synthetics for simple crustal models, and the *bottom three records* in dark line are observations. The differences between the two components of motion are caused by P to S converted phases generated by the structure under the station. The δ functions superimposed on the *top trace* mark the arrival time of the peak amplitude of the phases. The numbers 1 to 5 designate the phases P, $PpPmP$, $PpSmp$, Ps, $PpPms$ and $PpSms$, respectively. The relative height of the δ function indicates the strength of the arrival.

CRUSTAL STRUCTURE UNDER CAR

The problem of modeling the crustal structure under WWSSN station CAR is one which is well suited for study through the use of P to S and S to P converted phases. This is because of the stations ideal location with respect to several deep events in Argentina. The epicentral distance is about 39° and the orientation of the station is such that the N-S component is nearly purely radial and the E-W purely transverse. This eliminates the need for digitizing the records and resolving them into radial and transverse components. Also, it turns out that the crustal structure under CAR is very simple and easy to interpret.

The *top* of Figure 1 shows synthetic P wave forms computed for model CAR 1 in Table 1. This model represents a typical (Haskell, 1962) crustal layer over a half-

space with the properties of the lid. The crustal thickness and lid velocities have been adjusted so that the synthetics would match the three observations shown at the *bottom* of the figure. The relevant information on the size and location of the events is given in Table 2, and the range and azimuth data for CAR is given in Table 3.

TABLE 1
CRUSTAL MODELS FOR CAR

Model	Layer	*P* Velocity (km/sec)	*S* Velocity (km/sec)	Density (g/cc)	Thickness (km)
CAR 1	1	6.28	3.70	2.90	33.0
	2	8.10	4.68	3.70	—
CAR 2	1	6.28	3.70	2.90	33.0
	2	8.10	4.68	3.70	37.0
	3	7.60	4.10	3.47	—

TABLE 2
EVENT DATA

Source	Date	M_b	Lat.	Long.	Depth (km)
Argentina	1/17/67	5.5	27.4 S	63.3 W	590
Argentina	9/9/67	5.9	27.6 S	63.2 W	577
Argentina	8/23/68	5.8	22.0 S	63.5 W	537
Peru-Brazil	2/15/67	6.2	9.1 S	71.4 W	583
Peru-Brazil	11/3/65	6.1	9.1 S	71.3 W	598
Chile	12/27/67	6.3	21.3 S	68.2 W	135
Japan	1/19/69	6.3	44.9 N	143.2 E	238
New Hebrides	6/13/66	6.2	12.2 S	167.1 E	184

TABLE 3
STATION DATA

Station	Event	Date	Δ	Azimuth	Back Azimuth
CAR	Argentina	1/17/67	37.9	354.2	174.7
	Argentina	9/9/67	38.1	354.0	174.6
	Argentina	8/23/68	32.5	353.7	174.1
COR	Peru-Brazil	11/3/65	71.0	323.5	124.7
	Peru-Brazil	2/15/67	71.0	323.5	124.7
	Chile	12/27/67	82.6	323.8	129.5
	Japan	1/19/69	62.5	53.5	306.9
SFA	Argentina	9/9/67	74.7	354.6	173.0
SFA	Peru-Brazil	2/15/67	56.0	0.5	180.7
GWC	Argentina	9/9/67	83.5	351.7	167.0
SCH	Argentina	9/9/67	82.1	357.9	176.8
MNT	Argentina	9/9/67	73.4	352.4	170.4
MNT	Peru-Brazil	2/15/67	54.4	358.1	177.3
OTT	Argentina	9/9/67	73.5	350.1	168.4
OTT	Peru-Brazil	2/15/67	54.4	356.3	174.8
SCB	Peru-Brazil	2/15/67	53.1	352.9	170.3
LND	Peru-Brazil	2/15/67	52.6	351.0	167.8
TRN	Argentina	9/9/67	38.1	2.9	182.6
SJG	Argentina	9/9/67	45.5	356.1	176.3
SPA	New Hebrides	1/13/66	77.8	180.0	157.8

Note that the back azimuths to the events are all within 6° of being due south. The source used to compute the synthetics was a trapezoid with a zero-to-peak time of $\delta t_1 = 0.25$, a level peak time $\delta t_2 = 1.8$, and a peak-to-zero time $\delta t_3 = 0.2$ sec. Superimposed on the synthetic for model CAR 1 are a series of delta functions which mark the time of arrival of the peak amplitude of the rays which are first order in reflection or conversion coefficients from the discontinuity. The relative heights of the delta functions indicate the relative strength of the arrivals. The peak labeled 1 is the direct arrival; 2, the phase *PpPmp*, 3, the phase *PpSmp*; 4 the phase *Ps*, 5, the phase *PpPms*; and 6, the phase *PpSms*. Note that both in the synthetic and at corresponding points in the data, there is a clear difference between the vertical and radial components of motion, particularly when phases 5 and 6 arrive. It is also possible to see what appears to be a *PpPmp* arrival (phase 2) on the vertical components, but as was stated previously, it is impossible to distinguish it from a secondary source. It appears then that this very simple model gives a very adequate fit to the data except perhaps in the first backswing of the wave form where the data appears to peak up more sharply than the synthetic.

One simple way to correct this small discrepancy is to model the extra peak in the data as a *Ps* phase generated at the interface between the lid and the low-velocity zone. Model CAR 2 in Table 1 has been constructed to represent a typical crust and lid over a half-space with properties like the low-velocity zone (Helmberger, 1973). The corresponding synthetics are shown in Figure 1, and they do fit the data somewhat better. However, the features justifying the addition of this layer are relatively small, and there may be some other modifications of the model which would work as well. The important result is that the crust under CAR is about 33 km thick, and the transition between the crust and lid is relatively sharp. Generally speaking, the techniques discussed here are best suited for the study of the strongest and sharpest discontinuity in a given crustal column. This is, of course, almost always the Mohorovičić discontinuity. Model studies show that including a Conrad discontinuity in a crustal model has very little effect on the radial P wave form. A thick layer of soft sediment does have a visible effect, but very few seismic stations are situated on such layers.

The preceding discussion has shown that it is practical to use P to S converted arrivals in the radial P wave form for modeling crustal structure. It is important however, to find out how this method compares with the use of *Sp* arrivals in the *SV* wave forms. Figure 2 shows *SV* arrivals for the same three events as used in the P wave-form study. The *Sp* amplitudes predicted by model CAR 2 have been indicated. The first two records have *Sp* phases which correspond well to those predicted by model CAR 2. The third event, however, appears to have produced no *Sp* arrival at all. It has presumably been canceled out by the background level of other compressional arrivals. This type of noise is one of the largest drawbacks to the use of *Sp* phases because it introduces instability into the *Sp* amplitude. This means that it is necessary to compile a number of observations at a given station before the crustal structure can be modeled with a high level of confidence. However, this is probably true of P to S converted phases as well. The best approach would undoubtedly be to use both transmitted conversion data like *Sp* simultaneously with reflected conversion data like *PpPms*. The two types of information will not generally be compatible for a dipping interface. The use of both types of data corresponds in importance and information content with the reversal of profiles in refraction work.

Crustal Structure under COR

If the crustal structure under a station contains discontinuities which are pronounced enough, it is possible to distinguish both transmitted, converted phases and reflected, converted phases within the radial P component alone. One station which appears to be situated on a crust with some very sharp discontinuities is WWSSN station COR (Corvallis, Oregon). The *top traces* in Figure 3 are radial and vertical P observations at COR of a simple intermediate depth event (see Table 2) which occurred in Chile. The differences between the two components are very pronounced implying substation structure with large discontinuities.

COR was initially selected for study as a part of a more general investigation of the Puget-Willamette depression which is the structural province where it is located. The station is of importance here because of the strong effect of the crustal structure

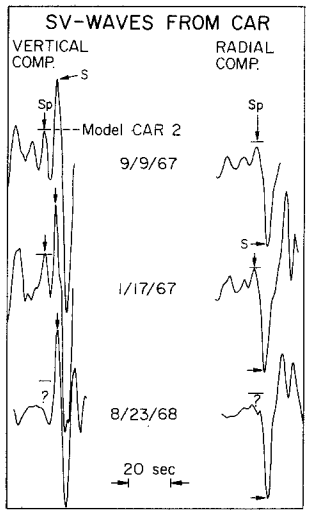

Fig. 2. The figure shows observed SV records at CAR for three different events which approached the station from similar azimuths. The first two events show a clear Sp phase. The amplitude for the phase predicted by model CAR 2 is shown as a short horizontal line segment. The third record contains no such arrival indicating the instability of the phase. When present, the Sp phase can be identified by its particle motion. It breaks the same way as direct S on the vertical component and opposite to S on the radial.

on the radial P wave forms. Accordingly, only a final model which explains those wave forms will be presented. A more detailed report on how the model was obtained and how it relates to the geology of the Puget-Willamette depression is in preparation. Another portion of the work which was a determination of the crustal structure from the body waves of the 4/29/65 Puget Sound earthquake has already been reported (Langston, 1977a).

A model for the crustal structure of the region was constructed by Berg *et al.* (1966) to fit long-range refraction observations at a group of stations including COR (see Table 4). The *bottom traces* in Figure 3 are synthetics computed using the model. The differences between the synthetic radial and vertical components are not nearly as large as between the observed radial and vertical components.

Figure 4 shows observations from COR of four different intermediate and deep events. As Table 3 shows, the signals approached the station from several different azimuths. The amplitude and shape of the secondary arrivals in the radial P wave form is relatively consistent. Since the station was not naturally rotated for any of

the arrivals, it was necessary to digitize the two horizontal records and rotate them into radial and transverse components. Only a very small signal appeared on the transverse component after rotation. There was no strongly anomalous particle motion as might be expected for severely dipping structure (Langston, 1977b).

On the *left* of Figure 4 are shown source functions which have been constructed by deconvolving the instrument from the observed vertical motion and matching the result with trapezoidal time functions. The source functions have been smoothed by

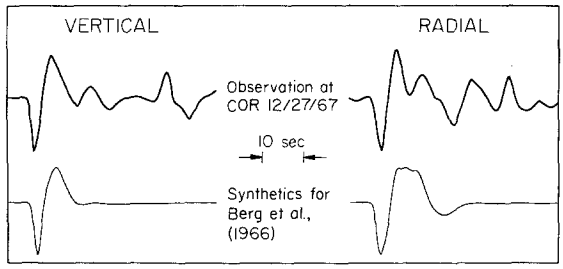

FIG. 3. The *top traces* are radial and vertical records of a simple event made at COR. The strong differences between the two components are caused by large amplitude P to S converted phases. The *bottom traces* are synthetics computed for a model of the crustal structure under COR which was proposed on the basis of refraction data. It is apparent that much stronger discontinuities exist in the Earth than in the model.

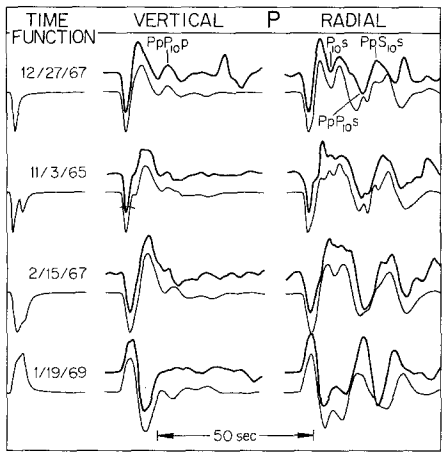

FIG. 4. The figure shows the two components of P-wave motion at COR for four different teleseismic events. The observed records are shown in dark line directly over synthetics for model COR 1 in light line. The source functions used in computing the synthetics are shown on the *left*. They have been convolved with the Q operator. The primary phases which originate at the strong discontinuity at the base of the shallow low-velocity zone (interface 10) are marked in the *top record*.

the Q operator so that the traces represent the wave form actually incident at the base of the crust. The source functions for the two Peru-Brazil events were modeled as sums of two lagged trapezoidal time functions because the deconvolutions showed that they were double events.

Under each of the observations in Figure 4 is a synthetic computed from model COR 1 which is listed in Table 4. The model was constructed by adding a low-velocity zone to a simplified version of the Berg *et al.* (1966) model and modifying the result to obtain a good fit. The final model is shown in Figure 5.

A strong case can be made from the observations for the sharp discontinuity at the

base of the low-velocity zone (45 km depth). Since this discontinuity is at the base of the tenth layer, phases which convert or reflect there are given a subscript 10. The transmitted conversion $P_{10}s$ and the reflected conversions $PpP_{10}s$ are marked in Figure 4. Also, there is an arrival in the vertical P observations which corresponds well with the $PpP_{10}p$ phase predicted by the model. There is, unfortunately, little direct evidence for the discontinuity at the top of the low-velocity zone since no strong arrivals appear to have originated at that depth. However, the Berg *et al.* (1966) refraction observations do show that there is a Pn velocity of 8.0 km/sec at depths as shallow as 15 km. This coupled with the observations of converted phases from a strong velocity increase of 1. to 1.5 km/sec at about 45 km depth implies that either the upper mantle P velocity is as high as 9.0 to 9.5 km/sec at this shallow depth or that there is a velocity reversal. The existence of a shallow low velocity in the Puget-Williamette depression has been confirmed in several different ways during the ongoing study of the region. Also, such a structure is consistent with much of

TABLE 4
CRUSTAL MODELS FOR COR

Model	Layer	P Velocity (km/sec)	S Velocity (km/sec)	Density (g/cc)	Thickness (km)
Berg *et al.* (1966)	1	4.4	2.5	2.5	2.2
	2	5.5	3.0	2.6	7.7
	3	6.6	3.8	2.8	3.8
	4	7.4	4.2	3.0	2.1
	5	8.0	4.6	3.2	10.0
COR 1	1	5.5	3.0	2.6	10.0
	2	6.7	3.9	2.8	6.0
	3	8.0	4.6	3.2	5.0
	4	7.9	4.5	3.15	1.5
	5	7.8	4.2	3.1	2.0
	6	7.7	3.7	3.0	1.5
	7	7.5	3.5	2.95	1.5
	8	7.2	3.3	2.9	2.0
	9	6.9	3.3	2.85	2.5
	10	6.6	3.3	2.85	12.9
	11	8.0	4.6	3.2	—

the refraction and gravity data reported by other authors for the region (Langston, 1976).

The rays generated at the other interfaces in the model are generally too small to be identified specifically in the theoretical wave form. However, the synthetics do match the strong variations in the observed radial P records for as much as 50 sec. The strong arrival late in the vertical P wave form of the 12/27/67 event is the pP phase which was not included in the calculated wave form.

The technique of comparing the radial P component to the vertical has proved particularly useful in this modeling study. This was because the discontinuity between layers 10 and 11 was large enough so that phase $P_{10}s$ was visible as well as $PpP_{10}s$ and $PpS_{10}s$. However, most cases will be like CAR where it is necessary to use SV waves to study transmitted, converted phases.

CRUSTAL STRUCTURE OF EASTERN CANADA

Jordan and Frazer (1975) used Sp phases in a study of the crustal structure of eastern Canada. They used records of a deep Peru-Brazil event (2/15/67) made at

seven stations scattered widely over the Superior and Grenville provinces. In so doing, they made the highly significant observation that they needed to include a broad low-shear-velocity zone in their model in order to fit the very large amplitudes of the Sp phases. As a starting model they used the crustal model of Massé (1973) which was based on P refraction data of the Canadian shield and surface-wave dispersion data from Brune and Dorman (1963). To satisfy the average $Sp - S$ travel time and the Sp amplitudes, they added an extra low-velocity layer at the base of the crust and slightly modified the parameters of the other layers so their final model

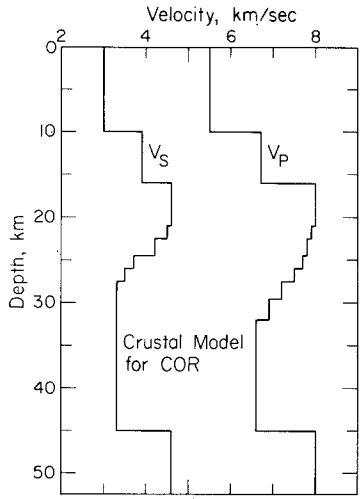

FIG. 5. This seismic profile (model COR 1) correctly predicts the observed P to S converted phases at COR. The phases generated by the strong interface at the base of the shallow low-velocity zone (interface 10 at 45 km depth) can be seen distinctly in the records.

TABLE 5
CRUSTAL MODELS FOR EASTERN CANADA

Model	Layer	P Velocity (km/sec)	S Velocity (km/sec)	Density (g/cc)	Thickness (km)
Massé (1973)	1	5.17	3.32	2.46	4.7
	2	6.22	3.65	2.81	17.1
	3	7.14	4.11	3.11	20.4
	4	8.06	4.65	3.41	
Jordan and Frazer (1975)	1	5.17	3.32	2.46	4.7
	2	6.22	3.65	2.81	10.3
JFFM	3	7.14	4.11	3.11	10.0
	4	6.80	3.40	3.11	10.0
	5	8.06	4.65	3.41	—

would also satisfy the dispersion data. Both their model and the Massé model are given in Table 5. These authors recognized the need for additional events and are preparing a more comprehensive report.

We present here a study of a deep Argentina event which provides some additional data of both the Sp type and the P to S converted type. This data shows that three of the seven stations do not seem to have a very sharp moho as far as reflections from the top side are concerned. Also, the variation in the crustal structure from station to station seem to be severe. It may not be appropriate to try to find one crustal structure which is valid for all of them.

Figure 6 shows P-wave observations of the deep Argentina event of 9/9/67 made at five different stations in eastern Canada. As in both the CAR study and the Jordan and Frazer (1975) study the NS component is nearly purely radial with respect to the event (see Table 3). A highly significant observation which can be easily made is that there is a great deal of variation in the radial components of the five stations while the vertical components are nearly identical. This indicates strong differences in crustal structure beneath the stations. The observations shown in Figure 1 can be used as a guide as to how reproducible the radial component can be expected to be, even for different events.

The synthetics for the Massé (1973) crustal model and for the Jordan and Frazer (1975) final model (JFFM) are also shown in Figure 6. As before, the phases *PpPms* and *PpSms* are of primary interest. The arrows in the figure mark the peak instru-

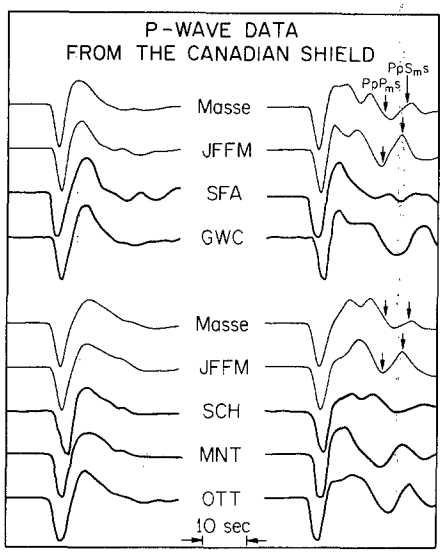

FIG. 6. Synthetics (light line) for the Massé and JFFM crustal models for the crustal structure in eastern Canada are compared with observations of the 9/9/67 deep Argentina event. The strong differences in the observed radial components from station to station indicates that no single crustal model would be appropriate for all of the stations. Stations SFA and SCH show only small *PpPms* and *PpSms* arrivals like those predicted by the Massé model. The other three stations show stronger arrivals but their travel times do not compare well with either model. The *top group of stations* are equipped with 15–100 instruments and the *bottom group* with 30–90 instruments.

ment response to the arrivals. Since the moho is less pronounced in the Massé model, the interference of arrivals from the upper crust with *PpPms* and *PpSms* appears to be much stronger. The two stations GWC and SFA are equipped with 15–90 instruments. At GWC the *PpSms* and *PpPms* phases are clearly visible and are approximately the same size as those predicted by JFFM. However, they arrive almost 5 sec late. This corresponds to a crustal column which is 14 to 19 km thicker than JFFM assuming a ray parameter of 0.05 sec/km. The radial component at SFA is almost an exact duplicate of the vertical. This observation is very difficult to correlate with the strong *Sp* precursor from the Peru-Brazil event unless the structure dips so that upgoing transmitted conversions are enhanced with respect to conversions reflected from the top side. The stations SCH, MNT and OTT have 30–90 instruments and are shown under the corresponding synthetics for the Massé (1973) and JFFM models. The record from SCH appears to match the synthetics for the Massé model very

closely. The moho does not appear to be nearly as sharp as in JFFM. Stations OTT and MNT appear to match the JFFM synthetics, particularly with respect to the phases *PpPms* and *PpSms*. There is, however, a significant difference in the first backswing of the two observed records. This means that there must be at least some differences in the crustal structure at MNT and OTT.

The refraction studies of Mereu and Jobidon (1971) and Berry and Fuchs (1973) have shown that the moho in eastern Canada has considerable topographic relief. This probably accounts for at least a portion of the variation in radial *P* waves between stations. Also there were strong variations in the *Pn* velocities observed by the aforementioned authors and by Rankin *et al.* (1969). This could be a further manifestation of topographic relief, of anisotropy, or of actual lateral variation of the composition of the lid in eastern Canada.

Unfortunately, none of the other deep Argentina events which occurred since installation of the Canadian network were large enough to produce usable radial *P* waves or vertical *SV* records. The 2/15/67 Peru-Brazil event already studied by Jordan and

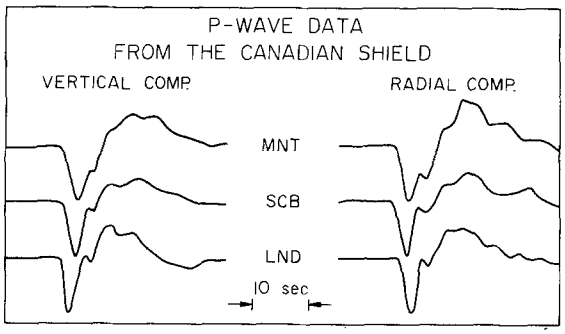

FIG. 7. These observed vertical *P* waves from the 2/15/67 Peru-Brazil event were too complex to model by using a sum of trapezoids as a source. A qualitative comparison of the vertical and radial components indicates that MNT contains strong *S* arrivals. Those in the SCB and LND records are much less pronounced.

Frazer (1975) produced large amplitude *P* waves but it had a long duration, multicomponent source. The vertical *P* waves could not be adequately modeled even by using a sum of two lagged trapezoids as in the COR study. Apparently, even more pulses were needed. The interaction of the later sources with the crustal phases from the first source proved to be very difficult to model. Also, at four of the seven stations the background noise was of the same size as the crustal phases in the radial *P* wave form. The three usable records are shown in Figure 7. Only a qualitative comparison can be made since the source could not be modeled. The vertical components are again very similar particularly at MNT and SCB which have identical instruments. There are relatively large differences between the radial and vertical components at MNT, just as there were for the deep Argentina event. At SCB the differences are not as pronounced indicating that the moho there is not as sharp. LND has very similar vertical and radial components just as did SFA. Until more records can be compiled, it will be impossible to make any definitive statement about the crustal structure under any of these stations. It does seem clear, however, that there are large differences in both moho sharpness and crustal thickness among the seven stations in the array.

The vertical component of the *SV* waves from the Peru-Brazil and Argentina events from stations OTT and SFA are compared in Figure 8. The *Sp* precursor at SFA was

larger than at any other station for the Peru-Brazil event, yet there is virtually no precursor at all at that station for the Argentina event. The Peru-Brazil event produced a double precursor at OTT. Jordan and Frazer (1975) interpreted the second of these as the one from the moho and the first as a conversion from some deeper discontinuity. The Argentina event appears to have the first precursor, but the *Sp* phase is again missing. The amplitude of the precursory phase seems to be a very unstable quantity. As shown by Langston (1976c), much of this instability can be accounted for by postulating a small dip on the moho. It would have been interesting to have compared the records from the two events at all seven stations. Unfortunately, most of them were at ranges where the precursor would be interfering with the *SKS* phase.

The data presented in this section is inadequate to discriminate between the JFFM

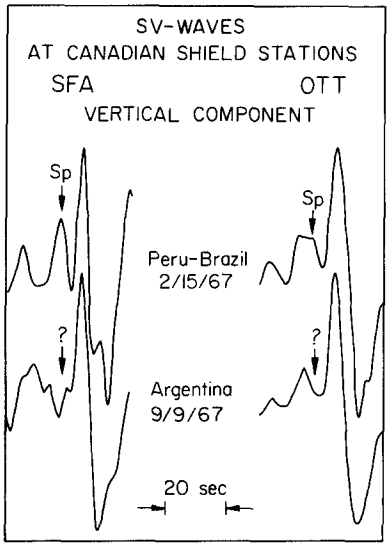

FIG. 8. The figure compares observed *Sp* phases from two different events at two different stations in the Canadian shield. The 2/15/67 event, the one studied by Jordan and Frazer (1975), produced strong *Sp* arrivals at both stations. They interpreted the second of the two precursors at OTT to be the one from the moho. The 9/9/67 event did not produce a strong *Sp* phase at either station even though it approached from a highly similar azimuth. There is obviously much instability in the amplitude of these phases.

and Massé models. It is not possible to say whether the low shear-velocity zone exists or not. The data does show, however, that there is much variation in crustal thickness and moho sharpness from station to station. There may be so much variation that a best average model for all the stations would not be particularly meaningful. The converted phases of both the S to P and P to S type appears to be so sensitive to the fine details of the crustal structure that the only viable approach may be to model each structure individually. Then any general features could be separated from the purely local ones.

ANOMALOUS STATIONS

One final advantage of the technique of comparing radial to vertical P observations in order to estimate the complexity of the crustal structure under the receiver is that it can be done quickly. Once several simple events from a given source region have been identified, it takes little time to determine whether the differences between the two components of displacement are small, moderate, or large at all stations within

30° to 80° of the events. Since the sharpest boundary is generally the moho, this usually amounts to determining whether the transition from crust to lid velocities is abrupt or graded. A survey of a large number of WWSSN stations was made to see if any correlations could be found between moho sharpness and tectonic setting. Stations from shield areas, stable continent, plate margins and oceanic islands were included in the study. However, it quickly became apparent that what was true in eastern Canada is true in general. The size and character of the arrivals in the radial P wave form varies greatly from station to station. If any general conclusion about a particular set of stations is to be reached, it must be done by modeling each station separately and looking for a common feature in the models.

In the course of the general survey, three stations were found where the effects of the substation structure appeared to be unusually severe. We are including the evidence for this in this paper because the information may be important when the stations are used in studies of other types. The first of these is station TRN (Trinidad

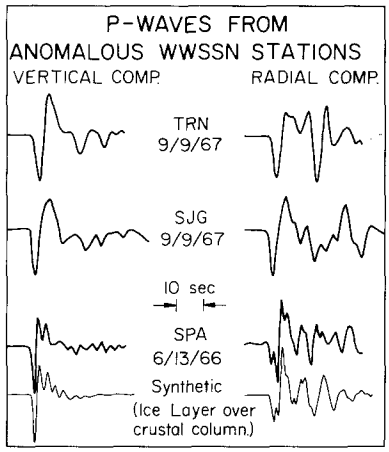

FIG. 9. The figure shows vertical and radial components of P-wave motion for simple events at three stations which are apparently situated on very complex structure. The synthetic under the SPA (South Pole Antarctica) record indicates that most of the distortion at that station is caused by the ice layer.

Port of Spain). The wave forms for the 9/9/67 Argentina event are shown at the top of Figure 9. The P to S converted phases are just as large as the direct arrival on the radial component. This means that pure P-mode crustal phases are probably distorting the vertical component as well. It would therefore be unwise to analyze the wave forms on either component without accounting for receiver structure.

The second highly anomalous station was SJG (San Juan, Puerto Rico). The wave forms for the 9/9/67 Argentina event are shown in the second row of Figure 9. There is a strong S arrival 30 sec after the direct. Attempts to model the arrival with reasonable plane-layered structure were highly unsuccessful. The records from the 2/15/67 and 11/3/65 events also contained this strong arrival. It has been observed that SH waves from deep Argentina events appear very complicated at SJG while they are very simple at the surrounding stations. As pointed out by Jordan and Frazer (1975), it is extremely difficult to distort SH waves with a reasonable, plane-layered receiver structure. It therefore seems likely that some of the structure under SJG has a significant dip.

The third trace in Figure 9 shows a record of a simple event taken at SPA (South

Pole Antarctica). The crustal phases are very large, even in the vertical component. Under the observation is a synthetic for a 3-km-thick ice layer over a crustal column. The ice layer is obviously the chief cause of the distortion of the vertical wave form. This is a problem which is certainly confined to stations located on the polar caps, but it is an interesting observation nonetheless.

Conclusions

This study has shown that using synthetic seismograms to model the S arrivals in the P wave form is a viable way to model the crustal structure under seismic stations. The technique has proved to be simple to use yet sensitive enough to yield important information about the structure under stations CAR, COR and under eastern Canada. Probably, the technique of modeling the truncated transfer ratio in the frequency domain could have been used with equal success, since the two methods employ the same basic information. The ultimate importance of the synthetic seismogram technique is that it will be easier to relate to other studies using synthetic seismograms. This type of study is playing an increasingly important role in current investigations of both the seismic source and the velocity structure of the mantle and core. In these studies, it is important to know which features of the wave form should be modeled as complications in the source or as structure in the velocity profiles, and which should not. An adequate understanding of the effects of receiver structure on the wave form is vital to answering this important question.

Acknowledgments

This research was supported by National Science Foundation Grant EAR76-06619.

References

Båth, M. and R. Stefánsson (1966). S – P Conversions at the base of the crust, *Ann. Geofis.* **19**, 119–130.

Berg, J. W., L. T. Trembly, D. A. Emilla, J. R. Hutt, J. M. King, L. T. Long, W. R. McKnight, S. K. Sarmah, R. Souders, J. V. Thiruvathukal, D. A. Vossler (1966). Crustal refraction profile, Oregon Coast Range, *Bull. Seism. Soc. Am.* **56**, 1357–1362.

Berry, M. J. and K. Fuchs (1973). Crustal structure of the Superior and Grenville provinces of the northeastern Canadian Shield," *Bull. Seism. Soc. Am.* **63**, 1393–1432.

Bonjer, K. P., K. Fuchs and J. Wohlenberg (1970). Crustal structure of the East African Rift system from spectral response ratios of long period body waves, *Z. Geophys.* **36**, 287–297.

Brune, J. and J. Dorman (1963). Seismic waves and earth structure in the Canadian Shield, *Bull. Seism. Soc. Am.* **53**, 167–210.

Fernandez, L. M. (1967). Master curves for the response of layered systems to compressional seismic waves, *Bull. Seism. Soc. Am.* **57**, 515–543.

Fernandez, L. M. and J. Careaga (1968). The thickness of the crust in Central United States from the spectrum of longitudinal seismic waves, *Bull. Seism. Soc. Am.* **58**, 711–741.

Futterman, W. I. (1962). Dispersive body waves, *J. Geophys. Res.* **67**, 5279–5291.

Hannon, W. J. (1964). An application of the Haskell-Thomson matrix method to the synthesis of the surface motion due to dilatational waves, *Bull. Seism. Soc. Am.* **54**, 2067–2079.

Haskell, N. A. (1960). Crustal reflection of plane *SH* waves, *J. Geophys. Res.* **65**, 4147–4150.

Haskell, N. A. (1962). Crustal reflection of plane P and SV waves, *J. Geophys. Res.* **67**, 4751–4767.

Helmberger, D. V. (1973). On the structure of the low-velocity zone, *Geophys. J.* **34**, 251–263.

Jordan, T. H. and L. N. Frazer (1975). Crustal and upper mantle structure from S_p phases, *J. Geophys. Res.* **80**, 1504–1518.

Kurita, T. (1973a). A procedure for elucidating fine structure of the crust and upper mantle from seismological data, *Bull. Seism. Soc. Am.* **63**, 189–209.

Kurita, T. (1973b). Regional variations in the structure of the crust in the Central United States from P-wave spectra, *Bull. Seism. Soc. Am.* **63**, 1663–1687.

Langston, C. A. (1976). Body wave synthesis for shallow earthquakes sources: Inversion for source and earth structure parameters, *Ph.D. Thesis*, California Institute of Technology.

Langston, C. A. (1977a) Corvallis, Oregon, crustal and upper mantle receiver structure from teleseismic *P* and *S* waves, *Bull. Seism. Soc. Am.* **67**, 713–724.

Langston, C. A. (1977b). The effect of planar dipping structure on source and receiver responses for constant ray parameter (in preparation).

Langston, C. A. and D. V. Helmberger (1975). A procedure for modelling shallow dislocation sources, *Geophys. J.* **42**, 117–130.

Leblanc, G. (1967). Truncated crustal transfer functions and fine crustal structure determination, *Bull. Seism. Soc. Am.* **57**, 719–733.

Leon, Lap Sau (1975). Crustal structure of the Baltic Shield beneath Umea, Sweden from the spectral behavior of long-period *P* waves, *Bull. Seism. Soc. Am.* **65**, 113–126.

Massé, R. P. (1973). Shear velocity beneath the Canadian Shield, *J. Geophys. Res.* **78**, 6943–6950.

Mereu, R. F. and G. Jobidon (1971). A seismic investigation of the crust and moho on a line perpendicular to the Grenville Front, *Can. J. Earth Sci.* **8**, 1553–1583.

Mikumo, T. (1971). Source processes of deep and intermediate earthquakes as inferred from long-period *P* and *S* wave forms, *J. Phys. Earth* **19**, 303–320.

Phinney, R. A. (1964). Structure of the Earth's crust from spectral behavior of long-period body waves, *J. Geophys. Res.* **69**, 2997–3017.

Rankin, D. S., R. Ravindra, and D. Zwicker (1969). Preliminary interpretation of the first refraction arrivals in Gaspé from shots in Labrador and Quebec, *Can. J. Earth Sci.* **6**, 771–774.

Seismological Laboratory
California Institute of Technology
Pasadena, California 91125

Division of Geological and Planetary Sciences
Contribution No. 2818

Manuscript received September 20, 1976